Femtosecond dynamics of $Cu(H_2O)_2$

Mark S. Taylor, Jack Barbera, Claus-Peter Schulz,[a] Felician Muntean,[b]
Anne B. McCoy,[c] and W. Carl Lineberger
JILA and Department of Chemistry and Biochemistry, University of Colorado, Boulder, Colorado 80309

(Received 3 September 2004; accepted 1 November 2004; published online 18 January 2005)

The ultrafast relaxation dynamics of $Cu(H_2O)_2$ is investigated using femtosecond photodetachment-photoionization spectroscopy. In addition, stationary points on the $Cu(H_2O)_2$ anion, neutral, and cation potential energy surfaces are characterized by *ab initio* electronic structure calculations. Electron photodetachment from $Cu^-(H_2O)_2$ initiates the dynamics on the ground-state potential energy surface of neutral $Cu(H_2O)_2$. The resulting $Cu(H_2O)_2$ complexes experience large-amplitude H_2O reorientation and dissociation. The time evolution of the $Cu(H_2O)_2$ fragmentation products is monitored by time-resolved resonant multiphoton ionization. The parent ion, $Cu^+(H_2O)_2$, is not detected above background levels. The rise to a maximum of the Cu^+ signal from $Cu^-(H_2O)_2$, and the decay of the $Cu^+(H_2O)$ signal from $Cu^-(H_2O)_2$ have similar $\tau \approx 10$ ps time dependences to the corresponding signals from $Cu^-(H_2O)$, but display clear differences at very short and long times. The experimental observations can be understood in terms of the following picture. Prompt dissociation of H_2O from nascent $Cu(H_2O)_2$ gives rise to a vibrationally excited $Cu(H_2O)$ complex, which dissociates to $Cu+H_2O$ due to coupling of H_2O internal rotation to the dissociation coordinate. This prompt dissociation removes all intra-H_2O vibrational excitation from the intermediate $Cu(H_2O)$ fragment, which quenches the long time vibrational predissociation to $Cu+H_2O$ previously observed in analogous experiments on $Cu^-(H_2O)$. © *2005 American Institute of Physics.* [DOI: 10.1063/1.1836759]

I. INTRODUCTION

The spectroscopic interrogation of gas-phase complexes has allowed investigation of phenomena such as the molecular interactions involved in the solvation of anions[1] and cations,[2,3] the solvent dynamics following solute excitation,[4–8] intermolecular energy transfer,[9,10] and the dynamics of a variety of unimolecular and bimolecular reactions.[5,7,11,12] We previously reported a femtosecond photodetachment-photoionization and quantum wave packet study of the solvent reorientation and dissociation dynamics within the $Cu(H_2O)$ complex following electron detachment from $Cu^-(H_2O)$,[13,14] and now extend the experimental investigation to $Cu(H_2O)_2$. We are interested in determining how the solvent reorientation and dissociation dynamics are affected by the addition of a second water molecule.

The femtosecond photodetachment-photoionization experiments reported here use a ~100 fs, 400 nm laser pulse to photodetach an electron from mass-selected $Cu^-(H_2O)_2$. Electron photodetachment from $Cu^-(H_2O)_2$ by one 400 nm photon (3.12 eV) produces neutral $Cu(H_2O)_2$ exclusively in its ground electronic state, as shown by negative ion photoelectron spectroscopy.[15–17] Chemical reaction of ground-state Cu with H_2O is strongly endothermic,[14] and so the dynamics investigated in these experiments is nonreactive. Electron photodetachment produces an ensemble of neutral $Cu(H_2O)_2$ complexes, far from their equilibrium geometry, and with internal energy comparable to the energy required for dissociation to $Cu+2H_2O$. As a result, nascent $Cu(H_2O)_2$ undergoes large-amplitude solvent rearrangement and dissociation. The time evolution of the daughter fragments of $Cu(H_2O)_2$ is monitored by time-delayed resonance enhanced multiphoton ionization (REMPI). This approach[13,18–22] affords many advantages over other femtosecond pump-probe methods. Starting with a negative ion allows mass selection; the electrostatic forces in the anion result in a well-defined range of neutral geometries at time zero; and photodetachment of a negative ion initiates the dynamics on the electronic ground-state potential energy surface of the neutral. Probing the time-evolving neutrals by REMPI affords both mass identification and simultaneous monitoring of the parent complex and its fragmentation products, and provides a probe that is sensitive to the instantaneous nuclear configuration of the neutral complexes.

As reported previously,[13,14,23] electron photodetachment from $Cu^-(H_2O)$ led to large-amplitude H_2O reorientation within and dissociation from $Cu(H_2O)$ due to the extreme difference in topology between the anion and neutral potential energy surfaces. $Cu^-(H_2O)$ has a hydrogen bonded (H-bonded) Cu^-–HOH configuration, while neutral $Cu(H_2O)$ has a more weakly bound interaction with a $Cu–OH_2$ minimum configuration. Electron photodetachment from $Cu^-(H_2O)$ produced an ensemble of vibrationally excited $Cu(H_2O)$ complexes with an average internal energy near the $Cu+H_2O$ dissociation threshold. *Ab initio* electronic

[a]Permanent address: Max-Born-Institüt für Nichtlineare Optik und Kurzzeitspektroskopie, Max-Born-Strasse 2A, D-12489, Berlin-Adlershof, Germany.
[b]Permanent address: Varian, Inc. Scientific Instruments, Walnut Creek, CA 94598.
[c]Permanent address: Department of Chemistry, The Ohio State University, Columbus, OH.

structure calculations and quantum wave packet calculations of the $Cu(H_2O)$ dynamics helped to confirm the following interpretations. Following electron photodetachment from $Cu^-(H_2O)$, rotation and angular delocalization of H_2O within the complex occurred faster than the 260 fs experimental time resolution. Dissociation of $Cu(H_2O)$ occurred on three different time scales, each separated by an order of magnitude. A fraction of the nascent $Cu(H_2O)$ complexes dissociated directly. The remaining bound complexes dissociated on a 10 ps time scale via coupling of H_2O internal rotation to the $Cu–H_2O$ dissociation coordinate, and on a 100 ps time scale by coupling of H_2O intramolecular vibrations to the $Cu–H_2O$ dissociation coordinate. Analogous direct dissociation and dissociation mediated via H_2O internal rotation were also identified in theoretical investigations of the dynamics of $Cl(H_2O)$ and $Br(H_2O)$ following electron photodetachment from their anions.[24,25]

The $Cu^-(H_2O)_2$ anion has been investigated by negative ion photoelectron spectroscopy[16,17] and *ab initio* calculations.[26] The experiment[16,17] employed a magnetic bottle electron spectrometer with an energy resolution of ~ 0.3 eV and obtained a vertical electron detachment energy of 1.95 eV, which allowed derivation of incremental H_2O dissociation energies of ~ 0.55 eV. The $Cu^-(H_2O)$ and $Cu^-(H_2O)_2$ photoelectron spectra have been recently remeasured with higher energy resolution in our laboratory, and the results will be reported in a forthcoming publication.[15]

The most striking finding from the present experiments is that no significant $Cu^+(H_2O)_2$ signal is observed. The rise to a maximum of the Cu^+ signal, and the decay of the $Cu^+(H_2O)$ signal display similar $\tau \approx 10$ ps time dependences to the corresponding signals from $Cu^-(H_2O)$,[13,14] yet display clear differences from the $Cu^-(H_2O)$ results at short and long times. The Cu^+ signal from $Cu^-(H_2O)_2$ does not show the pronounced short time behavior associated in the $Cu(H_2O)$ experiments[13] with direct dissociation to $Cu + H_2O$. In addition, the Cu^+ signal from $Cu^-(H_2O)_2$ does not display the long time rise, nor does the $Cu^+(H_2O)$ signal from $Cu^-(H_2O)_2$ display the long time decay, which were observed in the analogous signals arising from $Cu^-(H_2O)$.[13]

We structure the remainder of the paper as follows. Section II describes the experimental apparatus and techniques. In Sec. III, we describe the details of the *ab initio* electronic structure calculations. The experimental results are presented in Sec. IV. In Sec. V, we first present the results of the *ab initio* calculations, interpret the present $Cu(H_2O)_2$ experimental results in light of the $Cu(H_2O)$ results, and finally present a picture of the $Cu(H_2O)_2$ dynamics consistent with the present experimental results and *ab initio* calculations. In Sec. VI, we draw conclusions and recommend future investigations.

II. EXPERIMENT

The time-resolved photodetachment-photoionization of $Cu^-(H_2O)_2$ is performed using the charge-reversal instrument described previously,[13,20] so only relevant details will be given here.

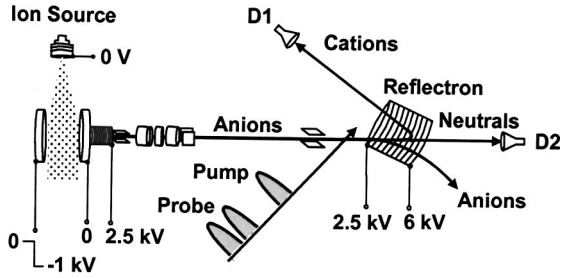

FIG. 1. Schematic diagram of the ion-beam part of the photodetachment-photoionization apparatus.

A. Ion production, transport, and product analysis

A schematic of the ion-beam part of the apparatus is presented in Fig. 1. A high-pressure pulsed sputtering discharge ion source[13,20] is used to make $Cu^-(H_2O)_n$ cluster ions. A mixture of 80% Ne and 20% Ar at stagnation pressures between 6–8 atm flows through a small water container at room temperature and expands into vacuum through a pulsed (200 Hz) General Valve (0.8 mm orifice). A sputtering discharge is initiated when the gas pulse flows between a copper rod cathode maintained at negative 2–3 kV and a stainless steel anode maintained at ground. The $Cu^-(H_2O)_2$ complexes are produced in the high-pressure region immediately following the discharge. They are further cooled and stabilized downstream, inside a conical expansion channel, and then allowed to expand into the $(0.5–1.0)\times 10^{-4}$ Torr pressure of the source chamber. Along with $Cu^-(H_2O)_n$ ions, the source generates Cu_n^-, $CuO^-(H_2O)_n$, $CuOH^-(H_2O)_n$, $O^-(H_2O)_n$, and $OH^-(H_2O)_n$. In order to avoid mass contamination of $^{63}Cu^-(H_2O)_2$ with $^{65}Cu(OH)_2^-$, we study the less abundant, but isotopically pure, m/z 101 ion packet, $^{65}Cu^-(H_2O)_2$. The rotational and vibrational temperatures of the anions made in this source are not well characterized. Previous studies of large cluster ions[27,28] indicated that they both range between 40 and 60 K. For these smaller clusters, we expect both to be higher, possibly 100–200 K.

Approximately 10 cm below the nozzle, a pulsed transverse electric field extracts the negative ions into a differentially pumped Wiley-McLaren[29] time-of-flight mass spectrometer (Fig. 1). They are further accelerated to ~ 3.3 keV energy, and brought to a spatial and temporal focus at the photodetachment region, 1.8 m downstream. The fast neutrals produced by photodetachment are detected by an in-line channeltron detector. The cation photoproducts enter a reflectron mass spectrometer and are subsequently counted with an off-axis microchannel-plate detector. This dual collector arrangement enables the normalization of the cation signal to the neutral signal, which is found to be very helpful for reducing the effects of fluctuations in the negative ion intensity and flight time.

B. Laser system

Most of the femtosecond laser system has been extensively described.[13,20,28] A Ti:sapphire oscillator (Coherent Mira Basic) pumped by a $Nd:VO_4$ laser (Coherent Verdi V5)

produces ~85 fs pulses at 750–850 nm. The pulses are amplified by a regenerative, multipass Ti:sapphire amplifier (Quantronix Titan), pumped by a Nd:YLF laser (Quantronix, model 527 DQ), to 3 mJ/pulse and 120 fs, at a repetition rate of 400 Hz. Two-thirds of this infrared light is used to generate second harmonic (400 nm) and third harmonic (267 nm) (CSK Optronics Supertripler, model 8315A) radiation, while the remainder pumps an optical parametric amplifier (OPA, Light Conversion TOPAS), whose fourth harmonic output provides tunable radiation between 300 and 400 nm. Finally, the OPA and the 400 nm pulses pass through delay stages and are further combined with the 267 nm pulse in a collinear configuration. All three pulses are focused to a spot of ~1 mm diameter at the point of interaction with the ion packet, where their typical energies are 100 μJ for 400 nm, 60 μJ for 267 nm, and 10–12 μJ for the OPA. Three-color, three-photon photodetachment-photoionization of Cu^- is used to determine the zero of time between the pump and probe pulses and to measure the time resolution of the experiments. A 400 nm pulse photodetaches an electron from Cu^- and a sequence of 327 and 267 nm photons resonantly ionize the $^2S_{1/2}$ Cu atom through the $^2P_{1/2}$ intermediate state. The delay between the excitation (OPA) and the ionization (267 nm) pulses is fixed at 0.3ps. As the photodetachment-resonant photoionization delay time Δt is varied, the Cu^+ signal exhibits a step function increase at $\Delta t = 0$. From fitting the time dependence of this step to a tanh function, we derive the time resolution of the experiments to be 260 fs.

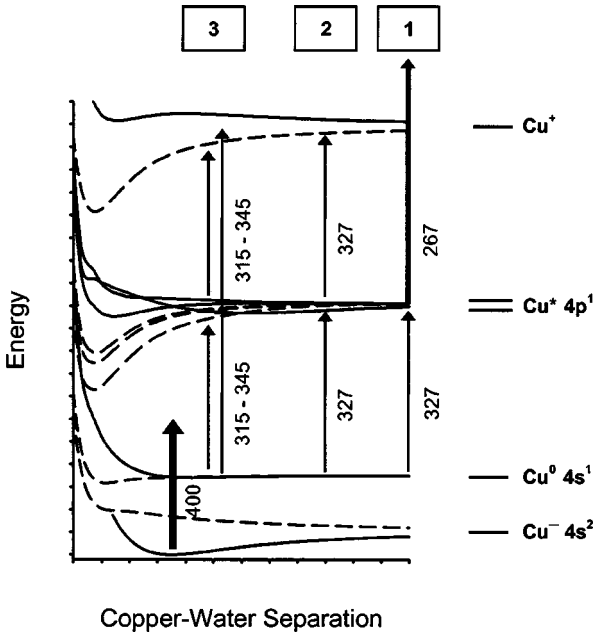

FIG. 2. Schematic representation of the measurements performed, superimposed on schematic $Cu(H_2O)_2$ anion, neutral, excited state, and cation potential energy curves. The figure is adapted from Refs. 13 and 23. Probe schemes 1–3 are discussed in the text.

C. Experimental details and data acquisition

A description of the various laser schemes used in the present photodetachment-photoionization experiments has been presented in detail,[13] and thus will be presented in brief here. All experiments form neutral $Cu(H_2O)_2$ by electron photodetachment from $Cu^-(H_2O)_2$ using a 400 nm pulse (Fig. 2). The dynamics are monitored by photoionizing $Cu(H_2O)_2$ and its fragments, Cu (Fig. 2, scheme 1) and $Cu(H_2O)$ (Fig. 2, schemes 2 and 3), and recording the resulting cation signals as a function of the delay between the photodetachment and the excitation/ionization pulses (OPA/267 nm). Different sets of experiments use OPA pulses tuned both on (327 nm) (Fig. 2, schemes 1 and 2) and off (315–340 nm) (Fig. 2, scheme 3) the Cu atomic $^2P_{1/2} \leftarrow {}^2S_{1/2}$ transition. Typical signal counts of $Cu^+(H_2O)$ and Cu^+ both vary between 0.1 and 0.2 counts/laser shot, while the $Cu^+(H_2O)_2$ two-color signal is too small to analyze.

Optimal laser-ion spatial overlap is achieved through the optimization of the photodetachment-photoionization of Cu^- in a two-step procedure. First, the photodetachment (400 nm) pulse is positioned in time and space to maximize the Cu neutral signal. The resonant excitation (327 nm) OPA and the ionization 267 nm pulses are introduced and adjusted spatially to maximize the Cu^+ cation signal. Care is taken to ensure that the laser modes are as uniform as possible in the region of interaction with the ions. Typically, 5%–10% of the parent negative ion beam is photodetached by the 400 nm radiation, but a significantly smaller proportion of the photodetached neutrals are themselves ionized by the subsequent pulses.

The data acquisition procedure consists of scanning a range of time delays between the 400 nm pulse and the fixed OPA and 267 nm pulses, while simultaneously measuring the neutral signal and the individual Cu^+, $Cu^+(H_2O)$, and $Cu^+(H_2O)_2$ product cation signals. One single scan consists of sweeping the entire range of time delays while data are accumulated during 800 laser shots per time delay. Many back and forth scans are performed, for a total of 20 000–40 000 laser shots per time delay. This procedure allows continuous monitoring of the measured signals at all time delays to allow correction for any major drift. The final signal (after appropriate background corrections) is given by the cation signal divided by the neutral signal. The principal challenge of the experiment arises from maintaining stability during the several hours of signal optimization and data acquisition. It is especially challenging to maintain a stable spatial overlap of the three laser beams and the ion packet due to the variations of the pulsed valve operation and the slight pointing drift of the three laser beams as the room temperature changes. Background signals due to the individual photodetachment or photoionization pulses are typically recorded at the beginning and end of data acquisition and are subtracted from the time-dependent signals. Error bars for the experimental data are obtained by comparing the scatter present in multiple data sets.

As part of the $Cu(H_2O)$ investigation,[13] we carried out photodetachment-photoionization experiments on $Cu^-(D_2O)$, and found, within the experimental uncertainties, the results of these to be identical to those from $Cu^-(H_2O)$. We thus do not carry out analogous $Cu^-(D_2O)_2$ experiments in the present investigation.

III. *AB INITIO* CALCULATIONS

Electronic structure calculations use the GAUSSIAN 98 and GAUSSIAN 03 program packages.[30,31] The ten core electrons and 19 valence electrons of copper are represented by a relativistic effective core potential and a $(7s,7p,6d,3f)$ valence basis set, together referred to as aug-SDB.[32] The Stuttgart-Dresden-Bonn (SDB) relativistic core potential and corresponding $(6s,5p,3d)$ basis set for Cu were developed by Preuss and co-workers.[33] In their study of anion and neutral CuX_2 $(X=\mathrm{Cl,Br})$, Wang and co-workers partially uncontracted and augmented the SDB valence basis set to yield the $(7s,7p,6d,3f)$ basis set that is used in the present study.[32] Hydrogen and oxygen are represented by augmented correlation-consistent polarized valence double and triple ζ basis sets, aug-cc-pVDZ and aug-cc-pVTZ.[34,35] Only the spherical harmonic components of the d and f functions are used ($5d$ and $7f$), which results in 79 basis functions for Cu, and 41 and 92 basis functions for H_2O for aug-cc-pVDZ and aug-cc-pVTZ, respectively.

All structures are optimized, using analytical gradients and second-order Møller-Plesset perturbation theory (MP2), with only valence electrons correlated. Geometries of stationary points are converged using the ''very tight'' gradient convergence criteria of Gaussian. The incremental dissociation energies from the minimum D_e and zero-point level D_0 of the anion, neutral, and cation $Cu(H_2O)_2$ complexes, the vertical detachment energy (VDE) of $Cu^-(H_2O)_2$, and ionization energy of $Cu(H_2O)_2$ at various geometries are evaluated using coupled cluster theory with single, double, and perturbative triple excitations, CCSD(T), correlating only the valence electrons.

When evaluating D_0, we use the zero-point vibrational energy calculated from the MP2 harmonic vibrational frequencies. The zero-point energy contribution from the H_2O vibrations is scaled by 0.96, while the zero-point energy contribution from the intermolecular modes is unscaled. We define the incremental dissociation energies for the anion, neutral, and cation complexes as

$$\mathrm{Cu(H_2O)} \rightarrow \mathrm{Cu} + \mathrm{H_2O} \quad D_0[\mathrm{Cu{-}H_2O}] \tag{1}$$

$$\mathrm{Cu(H_2O)_2} \rightarrow \mathrm{Cu(H_2O)} + \mathrm{H_2O} \quad D_0[\mathrm{Cu(H_2O){-}H_2O}]. \tag{2}$$

In our previous study of the anion, neutral, and cation $Cu(H_2O)$ complexes[23] we found that CCSD(T) in combination with aug-SDB accurately predicted selected atomic Cu properties such as the electron affinity and ionization potential. We also found that a larger H_2O basis set such as aug-cc-pVTZ was essential to provide an accurate description of the slight charge transfer and hydrogen bonding interactions between Cu^- and H_2O. We again use MP2/(aug-SDB aug-cc-pVTZ) for all geometry optimizations. The CCSD(T)/(aug-SDB aug-cc-pVTZ) calculations were intractable using our present computational resources, and so we report final energetics at the CCSD(T)/(aug-SDB aug-cc-pVDZ) level of theory. CCSD(T)/aug-cc-pVDZ and CCSD(T)/aug-cc-pVTZ both agree with the experimentally derived D_e of the water dimer of 0.23 eV,[36,37] which provides confidence in using CCSD(T)/(aug-SDB aug-cc-pVDZ). In line with our previous *ab initio* $Cu(H_2O)$ investigation,[23] we choose not to correct for possible effects of basis set superposition error on the $Cu(H_2O)_2$ anion, neutral, and cation complex dissociation energies.

IV. EXPERIMENTAL RESULTS

Two salient observations emerge from the photodetachment-photoionization experiments on $Cu^-(H_2O)_2$. First, the parent ion, $Cu^+(H_2O)_2$, is not detected above background levels. Second, the rise to a maximum of the Cu^+ signal from $Cu^-(H_2O)_2$ and the decay of the $Cu^+(H_2O)$ signal from $Cu^-(H_2O)_2$ have similar $\tau \approx 10$ ps time dependences to the corresponding signals from $Cu^-(H_2O)$. Before these results are presented, it is first essential to analyze the contributions that each laser color makes to the Cu^+ and $Cu^+(H_2O)$ signals. The $Cu^+(H_2O)_2$ counts are so low that analysis is precluded.

A. Laser contributions to the Cu^+ and $Cu^+(H_2O)$ signals

Figure 2 displays the photodetachment-photoionization laser schemes superimposed on a schematic $Cu(H_2O)_2$ potential-energy surface diagram. In the on-resonance (OPA = 327 nm) experiments, the Cu^+ signal has primarily a three-color (400 nm + 327 nm + 267 nm) dependence (Fig. 2, scheme 1). The major background in these experiments is produced by a two-color (327 nm + 267 nm) contribution, and is typically 10% of the maximum three-color signal. The $Cu^+(H_2O)$ signal has primarily a two-color (400 nm + OPA) dependence over the range of OPA wavelengths used (315–340 nm; Fig. 2, schemes 2 and 3). As in the $Cu(H_2O)$ experiments,[13,14] resonant intermediate states near the ionization threshold of $Cu(H_2O)$ make the 400 nm + OPA + OPA contribution to the $Cu^+(H_2O)$ signal much larger than the 400 nm + OPA + 267 nm component. One-color $Cu^+(H_2O)$ backgrounds arise from both the OPA and 400 nm pulses. The one-color $Cu^+(H_2O)$ backgrounds and the two-color $Cu^+(H_2O)$ signal increase with increasing laser beam intensity, and the one-color backgrounds can range to $\sim 50\%$ of the net counts. Before data collection, beam focusing and overlaps are optimized in order to maximize the two-color signal while minimizing the one-color backgrounds. Slight variation in laser overlaps and focusing leads to day-to-day variation in the Cu^+:$Cu^+(H_2O)$ ratio.

B. Time evolution of the Cu^+ and $Cu^+(H_2O)$ signals

Figure 3 shows the time evolution of the Cu^+ and $Cu^+(H_2O)$ signals arising from $Cu^-(H_2O)_2$, when 327 nm + 267 nm probe pulses are used. The rise of the Cu^+ signal and the decay of the $Cu^+(H_2O)$ signal are characterized by a $\tau \approx 10$ ps time constant and have reached their asymptotic values by $t \approx 50$ ps. The long time (100 ps) dissociation component observed in the $Cu(H_2O)$ experiments[13] is either absent, or contributes less than a few percent to the signals. Figure 4 shows that when the long time components are subtracted from the $Cu^-(H_2O)$ data,[13,38] there is excellent agreement between the Cu^+ and $Cu^+(H_2O)$ signals arising from $Cu^-(H_2O)$ and $Cu^-(H_2O)_2$.

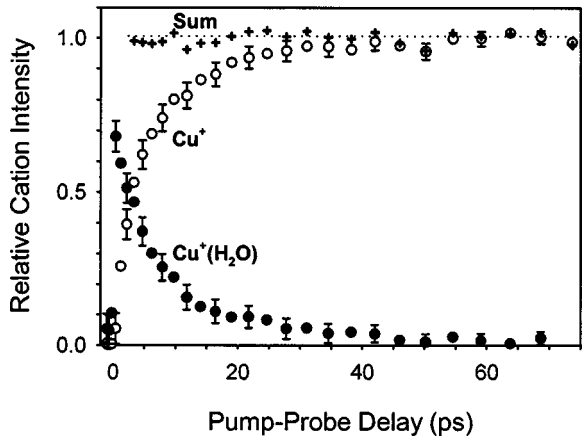

FIG. 3. Experimental time-dependence of the signals resulting from photodetachment-photoionization of $Cu^-(H_2O)_2$. The Cu^+ signal (hollow circles) is a result of 400 nm photodetachment followed by two-color (327 nm+267 nm) resonant ionization. The $Cu^+(H_2O)$ signal (black circles) is a result of 400 nm photodetachment followed by one-color (327 nm) resonant multiphoton ionization. The sum of the Cu^+ and $Cu^+(H_2O)$ signals is represented by crosses.

Figure 5 presents the onset of the Cu^+ and $Cu^+(H_2O)$ signals from $Cu^-(H_2O)_2$, when 327 nm+267 nm probe pulses are used. Superimposed for comparison are the Cu^+ and $Cu^+(H_2O)$ signals from $Cu^-(H_2O)$, along with the previously described fit to the Cu^+ signal from $Cu^-(H_2O)$,[13] and the time-zero t_0 of the experiment. The rise of the Cu^+ signal from $Cu^-(H_2O)_2$ is delayed by almost 1 ps from t_0, and the rapid rise observed in the Cu^+ signal from $Cu^-(H_2O)$ is either much smaller or not present. The $Cu^+(H_2O)$ signal from $Cu^-(H_2O)_2$ rises at the same rate as the instrument response and has a similar early time dependence to the $Cu^+(H_2O)$ from $Cu^-(H_2O)$.[13] The $Cu^+(H_2O)$ signal from $Cu^-(H_2O)_2$ appears to have a two-component decay and the proportion of the initial component ($t \approx 0-3$ ps) varies somewhat from data set to data set.

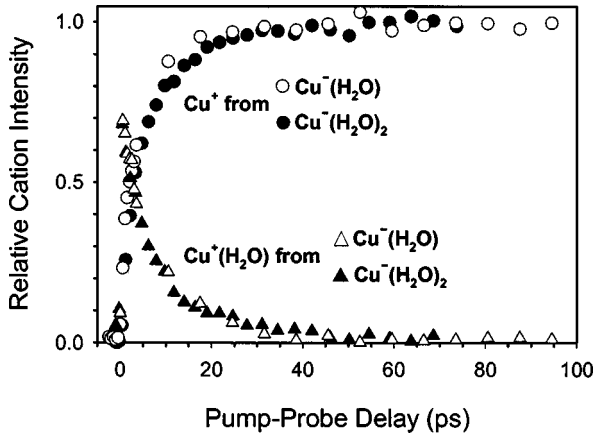

FIG. 4. Comparison of the signals obtained from photodetachment-photoionization experiments on $Cu^-(H_2O)$ (Cu^+: hollow circles and $Cu^+(H_2O)$: hollow triangles) and $Cu^-(H_2O)_2$ (Cu^+: black circles and $Cu^+(H_2O)$: black triangles). The measurements use the same photodetachment-photoionization laser scheme, as described in Fig. 3. The 100 ps component has been removed from the $Cu^-(H_2O)$ data as described in Ref. 38.

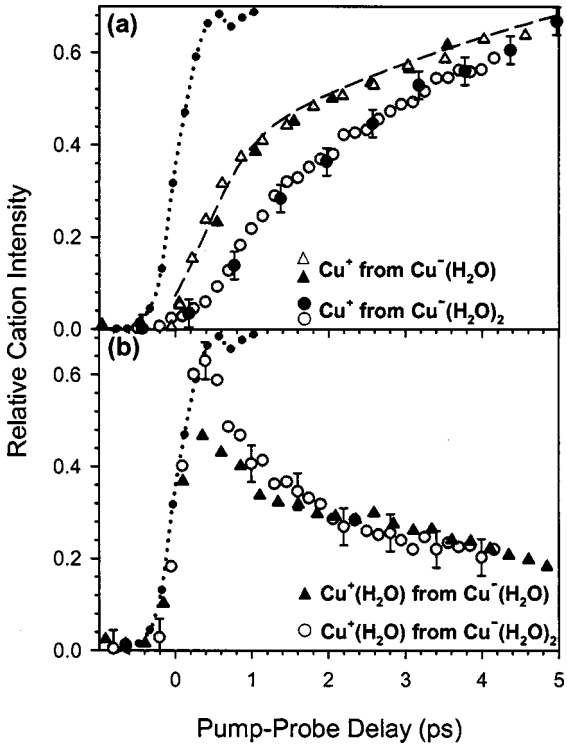

FIG. 5. Comparison of the experimental time dependence, in the first 5 ps after photodetachment, of (a) the Cu^+ signal resulting from $Cu^-(H_2O)$ (black and gray triangles) and $Cu^-(H_2O)_2$ (black and gray circles), and (b) the $Cu^+(H_2O)$ signal resulting from $Cu^-(H_2O)$ (black triangles) and $Cu^-(H_2O)_2$ (gray circles). The measurements use the same photodetachment-photoionization laser scheme as described in Fig. 3. The time-zero of the experiment is measured by the photodetachment-photoionization of Cu^- and is represented in both plots by a dotted line. A fit to the Cu^+ signal from $Cu^-(H_2O)$ (Ref. 38) is represented by a dashed line.

Experiments are also performed with the OPA probe pulse tuned from the 327 nm Cu $^2P_{1/2} \leftarrow {}^2S_{1/2}$ transition (OPA=315–340 nm), and with no 267 nm pulse present. The $Cu^+(H_2O)$ signals decay to zero similarly to the $Cu^+(H_2O)$ signals produced using OPA=327 nm. Some of these $Cu^+(H_2O)$ transients display clear structure in the first 3 ps following photodetachment. These features and the probe wavelength dependence of the $Cu^+(H_2O)$ signal will be investigated once colder anion temperatures are achieved.

V. RESULTS AND DISCUSSION

In order to develop a picture of the femtosecond dynamics of neutral $Cu(H_2O)_2$ and its fragmentation products, we interpret the present experimental results in the light of the previously investigated[13,14] dynamics of $Cu(H_2O)$ and *ab initio* electronic structure calculations on the $Cu(H_2O)_2$ anion, neutral, and cation complexes. We first examine the results of the *ab initio* calculations. Second, the previously reported $Cu(H_2O)$ results[13] are summarized. Finally, we interpret the $Cu(H_2O)_2$ results in light of similarities to and differences from the $Cu(H_2O)$ results, developing a full picture of $Cu(H_2O)_2$ dynamics that is consistent with all available information.

TABLE I. Energies of selected $Cu(H_2O)_2$ stationary points.

	CCSD(T) electronic energy[a] (eV)	CCSD(T) D_0 (eV)		Experimental D_0 (eV)	
Anion minimum	0.00	$D_0[Cu^- - H_2O]$	0.41	$D_0[Cu^- - H_2O]$	0.38 ± 0.02
$(\mathbf{1}^-, C_1)$		$D_0[Cu^-(H_2O) - H_2O]$	0.43	$D_0[Cu^-(H_2O) - H_2O]$	0.50 ± 0.02
Anion transition state	0.03		⋯		⋯
$(\mathbf{2}^-, C_2)$					
Anion transition state	0.12		⋯		⋯
$(\mathbf{3}^-, C_{2h})$					
Anion transition state	0.13		⋯		⋯
$(\mathbf{4}^-, D_{2d})$					
Neutral minimum	1.57	$D_0[Cu - H_2O]$	0.15		⋯
$(\mathbf{1}^0, C_1)$		$D_0[Cu(H_2O) - H_2O]$	0.28		⋯
Neutral transition state	1.97		⋯		⋯
$(\mathbf{2}^0, C_{2h})$					
Cation minimum	6.21	$D_0[Cu^+ - H_2O]$	1.73	$D_0[Cu^+ - H_2O]$	1.63 ± 0.08
$(\mathbf{1}^+, C_2)$		$D_0[Cu^+(H_2O) - H_2O]$	1.77	$D_0[Cu^+(H_2O) - H_2O]$	1.76 ± 0.07
Cation isomer	7.27	$D_0[Cu^+ - H_2O]$	1.73		⋯
$(\mathbf{2}^+, C_s)$		$D_0[Cu^+(H_2O) - H_2O]$	0.73		⋯

[a]Geometries are optimized at the MP2/(aug-SDB aug-cc-pVTZ) level of theory, and energies are calculated at the CCSD(T)/(aug-SDB aug-cc-pVDZ) level of theory.
[b]Experimental D_0s are derived from Refs. 16, 17, and 55.

A. *Ab initio* calculations

The *ab initio* calculations are divided into a discussion of the anion, neutral, and cation $Cu(H_2O)_2$ potential surfaces. Energies of selected anion, neutral, and cation $Cu(H_2O)_2$ stationary points are presented in Table I, their geometries in Fig. 6, and a schematic of the anion, neutral, and cation $Cu(H_2O)_2$ potential energy surfaces is presented in Fig. 7. Detailed geometrical parameters and harmonic frequencies of all stationary points are available from EPAPS.[39]

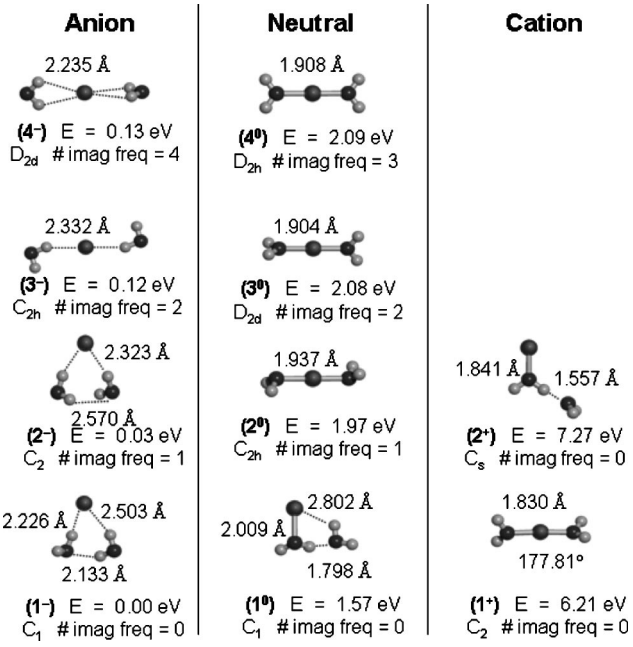

FIG. 6. $Cu(H_2O)_2$ anion, neutral, and cation stationary points optimized at the MP2(fc)/(aug-SDB aug-cc-pVTZ) level of theory. Electronic energy differences are calculated from the global minimum of the anion surface, at the CCSD(T)/(aug-SDB aug-cc-pVDZ) level of theory.

1. $Cu^-(H_2O)_2$ potential energy surface

Previous *ab initio* calculations on $Cu^-(H_2O)$ and $Cu^-(H_2O)_2$ have been reported by Iwata and co-workers.[26] Using MP2 with the 6-31G(d,p) basis set for H_2O and an all-electron $(10s,8p,4d,1f)$ basis set for Cu, they calculate a C_{2v} minimum for $Cu^-(H_2O)$, and for $Cu^-(H_2O)_2$, an ''in-

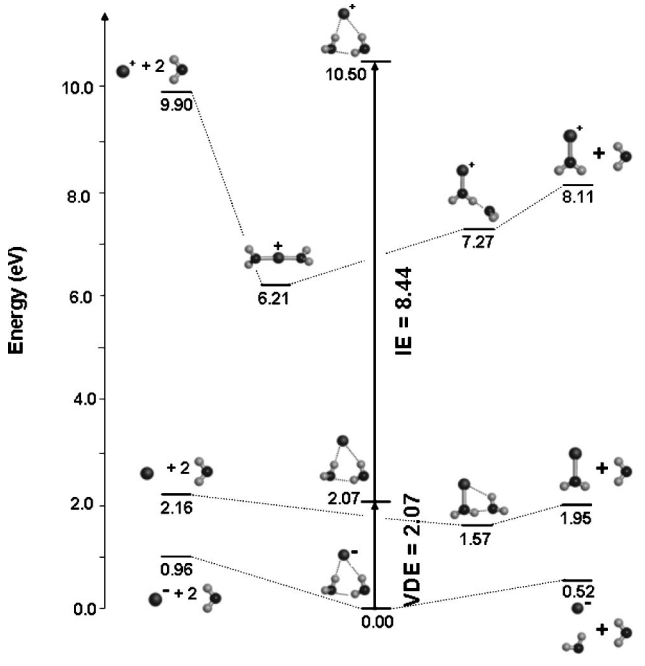

FIG. 7. Schematic of the anion, neutral, and cation $Cu(H_2O)_2$ potential energy surfaces. Stationary points are optimized at the MP2/(aug-SDB aug-cc-pVTZ) level of theory and final energies are calculated at the CCSD(T)/(aug-SDB aug-cc-pVDZ) level of theory. Energies are presented as the CCSD(T) electronic energy difference with respect to the $Cu^-(H_2O)_2$ minimum. The $Cu(H_2O)_2$ and $Cu^+(H_2O)_2$ structures at the anion equilibrium geometry are not stationary points on the neutral or cation potential energy surfaces.

ternal'' D_{2d} minimum possessing two equivalent waters and four equivalent Cu–H bonds. In contrast, our study of $Cu^-(H_2O)$ found that the larger aug-cc-pVTZ basis set for H_2O resulted in a C_s minimum, with one $Cu^- - HOH$ H-bond.[23] In order to establish the true global minimum for $Cu^-(H_2O)_2$, we carried out a thorough search of possible isomers using MP2/(aug-SDB aug-cc-pVTZ). We repeated this search using two other Cu basis sets: a 10 electron ECP and $(6s,5p,3d,2f,1g)$ valence basis set,[40] and a double-ζ all-electron basis set,[41] with aug-cc-pVTZ for H_2O. At the MP2/(aug-SDB aug-cc-pVTZ) level of theory, we find four stationary points (Fig. 6) and report their relative energetics at the CCSD(T)/(aug-SDB aug-cc-pVDZ) level of theory. They comprise a global minimum with a cyclic configuration ($\mathbf{1}^-$, C_1); a first-order transition state ($\mathbf{2}^-$, C_2) lying 0.03 eV above ($\mathbf{1}^-$); a second-order transition state ($\mathbf{3}^-$, C_{2h}) lying 0.12 eV above ($\mathbf{1}^-$); and a fourth-order transition state ($\mathbf{4}^-$, D_{2d}) lying 0.13 eV above ($\mathbf{1}^-$). Optimizations using the two other Cu basis sets did not locate an internal D_{2d} stationary point. We believe that the reported D_{2d} global minimum[26] is an artifact resulting from use of the 6-31G(d,p) basis set for H_2O, as this small basis set does not describe the $Cu^- - H_2O$ H-bonding interaction well.

Figure 6 shows the anion global minimum ($\mathbf{1}^-$) to have a cyclic structure, with two inequivalent H-bonds and one water-water H-bond. We label the water sharing the stronger H-bond with Cu^-, $H_2O^{(1)}$, and the other, $H_2O^{(2)}$. The $Cu^-(H_2O)_2$ minimum is similar in structure to that of $Cu^-(H_2O)$. The former has a $Cu^- - H$ bond length of 2.23 Å and $Cu^- - H - O$ angle of 160.8° in comparison to 2.33 Å and 156.7° in $Cu^-(H_2O)$. As in the $Cu^-(H_2O)$ complex, $H_2O^{(1)}$ and $H_2O^{(2)}$ have HOH that are angles compressed from the equilibrium value of 104.5° to 99.6° and 99.2°, respectively. The $Cu^- - H$ bonding interaction also lengthens the O–H bond length (of the H most closely bound to Cu^-) from 0.96 Å in free H_2O to 0.99 Å in the anion complex. We note that both IR spectroscopy[1,42,43] and *ab initio* calculations[44–51] show the $X^-(H_2O)_2$ (X=Cl,Br,I) complexes to have similar cyclic structures to the $Cu^-(H_2O)_2$ minimum, with two anion-water H-bonds and one water-water H-bond. We calculate $D_0[Cu^- - H_2O] = 0.41$ eV and $D_0[Cu^-(H_2O) - H_2O] = 0.43$ eV at the CCSD(T)/(aug-SDB aug-cc-pVDZ) level of theory. Using the measured vertical detachment energies of $Cu^-(H_2O)$ and $Cu^-(H_2O)_2$,[16,17,52] we derive $D_0[Cu^- - H_2O] = 0.38 \pm 0.02$ eV and $D_0[Cu^-(H_2O) - H_2O] = 0.50 \pm 0.02$ eV.

A deeper understanding of the $Cu(H_2O)_2$ dynamics will follow from knowledge of the range of anion geometries populated under the experimental conditions, as this defines the initial configurations of neutral $Cu(H_2O)_2$ at t_0. Infrared studies of gas-phase $X^-(H_2O)_2$ (X=F,Cl,Br,I) complexes have shown that the spectral signature of a water-water H-bond disappears when probing warmer clusters.[1,42,43] Additional insight is gained from a theoretical study of the temperature dependence of $Cl^-(H_2O)_2$ configuration by Watts and co-workers.[50] They found that for temperatures as low as 100 K, the water-water H-bond, present at 0 K, had broken as the complex sampled a wider range of configurations. The water-water H-bond in $Cu^-(H_2O)_2$ is distorted from that in the free water dimer (Fig. 6), with a H–O separation of 2.13 Å compared to 1.95 Å in the latter. We expect that this geometric distortion and the slight charge transfer from Cu^- to both water molecules weaken the water-water H-bond. Lying 0.03 eV (0.01 eV upon inclusion of zero-point vibrational energy) above ($\mathbf{1}^-$) is a first-order transition state ($\mathbf{2}^-$). In this transition state, rotation of the water molecules about the Cu–H axes has broken the water-water H-bond, while only increasing the O–O separation from that in ($\mathbf{1}^-$) by 0.12 to 3.13 Å. Estimating a $Cu^-(H_2O)_2$ vibrational temperature of 100–200 K,[53] we calculate a Boltzmann factor of $\sim 0.3-0.6$ for accessing ($\mathbf{2}^-$), which suggests that a fraction of $Cu^-(H_2O)_2$ will sample configurations without a water-water H-bond. The *ab initio* calculations indicate, however, that complete separation of the water molecules in transition state ($\mathbf{3}^-$) will cost ~ 0.12 eV. We thus expect that the $Cu^-(H_2O)_2$ produced and interrogated in the present experiments have two water molecules in close proximity.

We calculate a CCSD(T) vertical detachment energy of 2.07 eV for the $Cu^-(H_2O)_2$ minimum ($\mathbf{1}^-$), compared with 1.95 ± 0.3 eV measured by Fuke and co-workers.[16,17] We also calculate that the two $Cu^-(H_2O)_2$ stationary points ($\mathbf{3}^-$) and ($\mathbf{4}^-$) have electron detachment energies of 2.07 and 2.08 eV, respectively, which rules out the possibility of using the experimental $Cu^-(H_2O)_2$ vertical detachment energy to confirm the structure of the anion interrogated in the photoelectron spectroscopy experiments.

2. $Cu(H_2O)_2$ potential energy surface

Calculating accurate energetics and structures is more difficult for neutral $Cu(H_2O)_2$ than for the anion and cation complexes, due to its open electronic shell and lack of a charge center. An MP2 investigation of $Cu(H_2O)_2$ energetics by Curtiss and Bierwagen suggested that the complex has a $Cu - OH_2 - OH_2$ configuration in which the second water molecule H-bonds to the first rather than interacting with copper.[54] A thorough search for isomers using MP2/(aug-SDB aug-cc-pVTZ) (Figs. 6 and 7) reveals only one minimum on the neutral surface ($\mathbf{1^0}$). $D_0[Cu - H_2O]$ and $D_0[Cu(H_2O) - H_2O]$ are calculated to be, respectively, 0.15 and 0.28 eV, at the CCSD(T)/(aug-SDB aug-cc-pVDZ) level of theory. Three stationary points with $H_2O - Cu - OH_2$ configurations ($\mathbf{2^0}$, $\mathbf{3^0}$, $\mathbf{4^0}$) are located on the surface. These are not expected to play a role in the present $Cu(H_2O)_2$ dynamics as they are, respectively, 0.02, 0.13, and 0.14 eV in electronic energy above the energy of dissociated $Cu(H_2O) + H_2O$.

Figure 7 shows that the electronic energy of neutral $Cu(H_2O)_2$ at the anion equilibrium geometry is 0.50 eV higher than that of the minimum ($\mathbf{1^0}$), 0.11 eV above that of dissociated $Cu(H_2O) + H_2O$, while still 0.09 eV below that of dissociated $Cu + 2H_2O$. Based on the harmonic frequencies of the anion,[39] we estimate that nascent $Cu(H_2O)_2$ is born with up to ~ 0.1 eV of kinetic energy in intermolecular modes, which is sufficient to dissociate to $Cu + 2H_2O$. We calculate the ionization energy of neutral $Cu(H_2O)_2$ at the anion geometry to be 8.44 eV.

3. $Cu^+(H_2O)_2$ potential energy surface

We locate two minima on the $Cu^+(H_2O)_2$ surface (Figs. 6 and 7). The global minimum ($\mathbf{1}^+$, C_2) has a H_2O–Cu–OH_2 configuration, with an O–Cu–O angle of 177.81°. At the CCSD(T)/(aug-SDB aug-cc-pVDZ) level of theory, $D_0[Cu^+-H_2O]$ and $D_0[Cu^+(H_2O)-H_2O]$ are calculated to be 1.73 and 1.77 eV, respectively. These values are in good agreement with the $D_0[Cu^+-H_2O]=1.63\pm0.08$ eV and $D_0[Cu^+(H_2O)-H_2O]=1.76\pm0.07$ eV measured by collision-induced dissociation.[55] Several recent *ab initio* studies of the binding of H_2O to Cu^+ have likewise found that the second H_2O binds more strongly to Cu^+ than the first; and this effect has been explained using Cu^+ orbital hybridization arguments.[56–60] Lying 1.07 eV above the global minimum is a C_s isomer ($\mathbf{2}^+$) with a Cu–OH_2–OH_2 configuration. $D_0[Cu^+(H_2O)-H_2O]$ for ($\mathbf{2}^+$) is calculated to be 0.73 eV. The electronic energy of the $Cu^+(H_2O)_2$ at the anion equilibrium geometry lies 4.30 eV above that of the global minimum ($\mathbf{1}^+$), 2.39 eV above that of $Cu^+(H_2O)+H_2O$, and 0.61 eV above that of the completely dissociated Cu^++2H_2O, and so it is expected, in the current experiments, that both dissociation channels are open to $Cu^+(H_2O)_2$.

B. Cu(H_2O) dynamics revisited

Before proceeding with a detailed discussion of the results of the $Cu(H_2O)_2$ experiments, we summarize the findings of the $Cu(H_2O)$ dynamics. In that earlier study,[13,14,23] calculations showed that $Cu^-(H_2O)$ is delocalized between two equivalent H-bonded Cu^-–HOH configurations, with the HOH angle compressed to ~99°. Electron photodetachment from this anion resulted in a $Cu(H_2O)$ wave packet with average energy sufficient to dissociate to $Cu+H_2O$. A fraction of the wave packet dissociated directly. The neutral potential surface was found to be relatively flat at the anion Cu–H_2O separation, and as a consequence, the zero-point energy associated with $Cu^-(H_2O)$ bending was converted into quasifree rotation of H_2O within $Cu(H_2O)$. Over a period of several picoseconds, this internal rotation of H_2O was converted into Cu–H_2O dissociation, with a characteristic time constant of $\tau=8$ ps. A slower, $\tau=100$ ps, dissociation component was identified. This component (~15%) was suggested to arise from vibrational predissociation driven by intra-H_2O vibrations. Recent photoelectron spectroscopy experiments from our laboratory[15] are completely consistent with this conclusion.

C. Cu(H_2O)$_2$ dynamics

The salient observations from the $Cu(H_2O)_2$ experiments are first, that the parent cation, $Cu^+(H_2O)_2$, is not observed and second, that the Cu^+ and $Cu^+(H_2O)$ signals resulting from $Cu^-(H_2O)_2$ show similar time dependences to those from $Cu^-(H_2O)$ (Figs. 3 and 4). First, we consider the neutral species that gives rise to these Cu^+ and $Cu^+(H_2O)$ signals. The time dependence, and the 327 nm + 267 nm laser dependence of the Cu^+ signal suggests that it arises from ionization of an increasing population of neutral copper atoms. The time dependence of the $Cu^+(H_2O)$ signal suggests that it arises from ionization of a decaying population of either neutral $Cu(H_2O)$ (Ref. 13) or $Cu(H_2O)_2$ complexes,[61] and these two possibilities can result from either a concerted or stepwise dissociation of $Cu(H_2O)_2$:

$$Cu(H_2O)_2 \rightarrow Cu+2H_2O, \tag{3}$$

$$Cu(H_2O)_2 \rightarrow Cu(H_2O)+H_2O \rightarrow Cu+2H_2O. \tag{4}$$

The concerted dissociation of $Cu(H_2O)_2$ [Eq. (3)] seems improbable, based upon the observed time dependences of the Cu^+ and $Cu^+(H_2O)$ signals. To give rise to the observed Cu^+ and $Cu^+(H_2O)$ signals, the concerted dissociation would have to occur on a time scale almost identical to that measured for the dissociation of $Cu(H_2O)$ from $Cu^-(H_2O)$. Moreover, the absence of $Cu^+(H_2O)_2$ signal requires that all $Cu^+(H_2O)_2$ dissociates to $Cu^+(H_2O)+H_2O$ following ionization. Accordingly, it is most likely that the $Cu(H_2O)_2$ dissociation is stepwise [Eq. (4)], proceeding through a short-lived $Cu(H_2O)$ intermediate, which dissociates to $Cu+H_2O$ on a $\tau\approx10$ ps time scale. To understand the dynamics of this stepwise dissociation, we examine the results of the experiments and the *ab initio* calculations.

1. Early time $Cu(H_2O)_2$ dynamics

Immediately following photodetachment, the $Cu(H_2O)_2$ complexes will have two adjacent water molecules, with a fraction of the complexes containing a water-water H-bond. The two water molecules no longer experience the strong attraction to copper as they did in the anion complex, and so by analogy with $Cu(H_2O)$,[13,14] we expect that the intermolecular bending vibrations present in $Cu^-(H_2O)_2$ will give rise to rapid rotation of both water molecules within $Cu(H_2O)_2$. This prediction is supported by the observation of the immediate onset of $Cu^+(H_2O)$ from $Cu^-(H_2O)_2$ (Fig. 5). The calculated vertical ionization potential of $Cu(H_2O)_2$ at the anion geometry is 8.44 eV, greater than the 7.30–7.88 eV carried by two 315–340 nm photons. This suggests that within the 260 fs experimental resolution, one or both water molecules have reoriented within the complex such that O is pointing toward Cu, and the ionization energy is accessible with the absorption of two 315–340 nm photons. Based on the harmonic frequencies of the anion,[39] we estimate that nascent $Cu(H_2O)_2$ is born with up to ~0.1 eV of kinetic energy in intermolecular modes. It is thus likely that the H_2O reorientation will break the ~0.10 eV water-water H-bond, present in a fraction of the nascent $Cu(H_2O)_2$, and even result in a water-water collision with a consequent prompt H_2O dissociation. Assuming two limits of 50 and 1000 cm^{-1} for the translational energy of the separating fragments, we estimate that in the first 260 fs after t_0, $Cu(H_2O)$ and H_2O will only separate by 0.7 and 3.3 Å, respectively. This suggests that for very early times, the absorbing species is $Cu(H_2O)_2$ which, upon photoionization, does not remain bound as $Cu^+(H_2O)_2$.

Another clue concerning the early time dynamics of $Cu(H_2O)_2$ is revealed in the onset of the Cu^+ signal. Figure 5 shows that unlike the Cu^+ signal arising from $Cu^-(H_2O)$, there is little or no fast ($\tau<1$ ps) component observed in the Cu^+ signal arising from $Cu^-(H_2O)_2$. In the $Cu(H_2O)$

study,[13] we interpreted this component of the Cu^+ signal to arise from direct dissociation of $Cu(H_2O)$. The ~500 fs delay of the Cu^+ signal onset was interpreted as the time necessary for the wave packet to travel from the initial anion separation $R \approx 3$ Å to $R > 7$ Å, where two-color, 327 nm + 267 nm, resonant ionization produced Cu^+. Both quantum wave packet and simple classical calculations suggested that this fast direct dissociation component arose from that fraction of $Cu^-(H_2O)$ having Cu–H_2O stretch excitation. Two possibilities could explain the lack of this fast dissociation of $Cu(H_2O)_2$ to $Cu + 2H_2O$. First, the precursor $Cu^-(H_2O)_2$ may be vibrationally cooler than $Cu^-(H_2O)$, and thus lack a significant population having the Cu–H_2O stretch excitation necessary to produce direct dissociation. We discount this. Both $Cu^-(H_2O)$ and $Cu^-(H_2O)_2$ are produced by similar ion source conditions, have similar H_2O dissociation energies and similar Cu–H_2O stretching frequencies. Accordingly, we expect $Cu^-(H_2O)$ and $Cu^-(H_2O)_2$ to have similar populations of excited Cu–H_2O stretching vibrations. Most probable is that the water-water interaction in nascent $Cu(H_2O)_2$ quenches the direct dissociation to $Cu + 2H_2O$.

A final clue concerning the early time $Cu(H_2O)_2$ dynamics is that the Cu^+ and $Cu^+(H_2O)$ signals arising from $Cu^-(H_2O)_2$ do not display the long time dissociation component present in the $Cu^-(H_2O)$ data (Fig. 3). This component was interpreted to arise from vibrational predissociation to $Cu + H_2O$, driven by intra-H_2O vibrations.[13] Electrostatic forces result in compression of the HOH angle from 104.5° to ~99° in $Cu^-(H_2O)$,[23] and in both water molecules in $Cu^-(H_2O)_2$. As a consequence of this distortion, electron photodetachment from $Cu^-(H_2O)$ results in ~10% of neutral $Cu(H_2O)$ and $Cu(H_2O)_2$ complexes containing a water molecule with one quantum of HOH bend.[15] We suggest that rapid dissociation of the first H_2O from $Cu(H_2O)_2$ removes all intra-H_2O vibrational excitation from the daughter $Cu(H_2O)$ fragment, thus quenching the long time vibrational predissociation of $Cu(H_2O)$.

2. Longer time $Cu(H_2O)_2$ dynamics

Finally, we consider the dynamics of the $Cu(H_2O)$ intermediate resulting from dissociation of the first water molecule from $Cu(H_2O)_2$. Figures 3 and 4 show that this intermediate continues dissociating to $Cu + H_2O$ on a similar, $\tau \approx 10$ ps, time scale to that observed in the $Cu^-(H_2O)$ experiments.[13] In the earlier experiments, this dissociation was shown to arise from coupling of H_2O internal rotation to the Cu–H_2O dissociation coordinate, and we apply the same picture to the $Cu(H_2O)$ intermediate from $Cu^-(H_2O)_2$. *Ab initio* calculations suggest that internal rotational excitation of H_2O results in a dynamically averaged band of $^2P \leftarrow {}^2S$ excitation energies.[14,23] Rotational excitation of H_2O within the present $Cu(H_2O)$ intermediate is thus supported by the observation that the $Cu^+(H_2O)$ signals arising from $Cu^-(H_2O)_2$ show similar time decays when probed using 315–340 nm.

VI. CONCLUSIONS

We report femtosecond photodetachment-photoionization experiments which give direct insight into the dynamics of the vibrationally excited neutral $Cu(H_2O)_2$ complex and its fragmentation products following electron photodetachment of $Cu^-(H_2O)_2$. In addition, we present detailed *ab initio* electronic structure calculations on the anion, neutral, and cation charge states of $Cu(H_2O)_2$, which aid in interpreting the experiments. The experiments use a 400 nm, 100 fs laser pulse to photodetach an electron from mass-selected $Cu^-(H_2O)_2$, which produces a neutral $Cu(H_2O)_2$ complex in its ground electronic state, far from its equilibrium geometry, and with average internal energy comparable to the energy for dissociation to $Cu + 2H_2O$. As a result, nascent $Cu(H_2O)_2$ undergoes large-amplitude solvent rearrangement and dissociation. The time evolution of the daughter fragments of $Cu(H_2O)_2$ is monitored by time-delayed resonance enhanced multiphoton ionization.

Ab initio calculations predict that there is only one minimum on the $Cu^-(H_2O)_2$ potential surface. This minimum possesses a cyclic structure, with two inequivalent Cu^-–water H-bonds and one water-water H-bond. Calculations suggest that neutral $Cu(H_2O)_2$ has just one minimum, with a H-bonded Cu–OH_2–OH_2 configuration, and that regions of the surface with H_2O–Cu–OH_2 configurations lay above the energy of dissociated $Cu(H_2O) + H_2O$. Neutral $Cu(H_2O)_2$ at the anion equilibrium geometry is calculated to have average internal energy sufficient to dissociate to $Cu + 2H_2O$. This suggests that, in the present experiments, $Cu(H_2O)_2$ can dissociate through both $Cu(H_2O) + H_2O$ and $Cu + 2H_2O$ channels. $Cu^+(H_2O)_2$ is calculated to have a global minimum with H_2O–Cu–OH_2 configuration, and a second minimum with H-bonded Cu–OH_2–OH_2 configuration.

Most strikingly, a signal corresponding to the $Cu^+(H_2O)_2$ parent cation is not observed in the present experiments. The rise to a maximum of the Cu^+ signal from $Cu^-(H_2O)_2$, and the decay of the $Cu^+(H_2O)$ signal from $Cu^-(H_2O)_2$ have similar $\tau \approx 10$ ps time dependences to the corresponding signals from $Cu^-(H_2O)$, but display clear differences at very short and long times. Unlike the Cu^+ signal arising from $Cu^-(H_2O)$, the Cu^+ signal from $Cu^-(H_2O)_2$ does not show a fast ($\tau < 1$ ps) onset. Another difference is that neither the Cu^+ or $Cu^+(H_2O)$ transients arising from $Cu^-(H_2O)_2$ show the significant long time (100 ps) component observed in the $Cu^-(H_2O)$ experiments. We present the following dynamical picture which is consistent with the negligible counts of $Cu^+(H_2O)_2$, and the lack of significant short and long time dissociation channels in the Cu^+ and $Cu^+(H_2O)$ transients. Electron photodetachment from $Cu^-(H_2O)_2$ converts anion intermolecular vibrational motion into large-amplitude reorientation of the water molecules within neutral $Cu(H_2O)_2$. This results in a water-water collision with consequent prompt dissociation of the first water molecule. The prompt dissociation leaves a vibrationally excited $Cu(H_2O)$ complex, which undergoes dissociation via coupling of H_2O internal rotation to the Cu–H_2O dissociation coordinate. In the present $Cu^-(H_2O)_2$ experiments, we suggest that prompt dissociation of H_2O from nascent $Cu(H_2O)_2$ removes all intra-H_2O vibrational excitation

from the intermediate $Cu(H_2O)$ fragment, which quenches the long time vibrational predissociation to $Cu+H_2O$ previously observed in the $Cu^-(H_2O)$ experiments.

The results of this study invite several future investigations. At present, we are working on producing colder anions by tagging anion complexes with rare gas atoms and by experimenting with entrainment sources to introduce the neutral ligands.[1,62] Theoretical investigation of the dynamics of $Cu(H_2O)_2$ following photodetachment of its anion will complement this experimental study and deepen our understanding of the dynamics. We also hope to extend these investigations to more extensively solvated anion complexes, to aid the understanding of bulk solvation phenomena, particularly the solvation dynamics following photodetachment of anions in solution.[63–68] Another compelling set of experiments would investigate the time-resolved solvent rearrangement dynamics following excitation of a charge transfer state in a cluster anion.[69–72]

ACKNOWLEDGMENTS

The authors are pleased to acknowledge support from the National Science Foundation under Grant Nos. IGERT (J.B.), CHE0200968 (A.B.M.), CHE0201848 and PHY0096822 (W.C.L.), and the Air Force Office of Scientific Research Grant No. F49620-02-1-0371 (W.C.L.). A.B.M. also acknowledges the Dreyfus Foundation awards program for partial support of this work. C.P.S. was supported by the JILA Visiting Fellowship program. Electronic Structure Calculations were performed on the JILA Keck cluster, for which the authors acknowledge support from the W. M. Keck Foundation. M.S.T. is grateful for helpful conversations and correspondence with Dr. Pavel Jungwirth and Dr. Martina Roeselová.

[1] W. H. Robertson and M. A. Johnson, Annu. Rev. Phys. Chem. **54**, 173 (2003).
[2] M. A. Duncan, Int. Rev. Phys. Chem. **22**, 407 (2003).
[3] M. A. Duncan, Annu. Rev. Phys. Chem. **48**, 69 (1997).
[4] D. M. Neumark, Annu. Rev. Phys. Chem. **52**, 255 (2001).
[5] Q. Zhong and A. W. Castleman, Jr., Chem. Rev. (Washington, D.C.) **100**, 4039 (2000).
[6] R. Parson, N. Delaney, A. Sanov, and W. C. Lineberger, in *Physics and Chemistry of Clusters, Proceedings of Nobel Symposium 117*, edited by E. E. B. Campbell and M. Larsson (World Scientific, Singapore, 2001), p. 132.
[7] T. E. Dermota, Q. Zhong, and A. W. Castleman, Chem. Rev. (Washington, D.C.) **104**, 1861 (2004).
[8] A. Sanov and W. C. Lineberger, PhysChemComm **5**, 165 (2002).
[9] Z. Bačiá and R. E. Miller, J. Phys. Chem. **100**, 12945 (1996).
[10] I. V. Hertel, C. Bobbert, C. P. Schulz, P. Farmanara, H.-H. Ritze, V. Stert, and W. Radloff, in *Nobel Symposium 117*, edited by E. E. B. Campbell and M. Larsson (World Scientific Publishing Co., Visby, Sweden, 2000), p. 180.
[11] C. Wittig and A. H. Zewail, in *Chemical Reactions in Clusters*, edited by E. R. Bernstein (Oxford University Press, New York, NY, 1996), p. 64.
[12] J. A. Syage and A. H. Zewail, Adv. Mol. Vib. Collision Dyn. **3**, 1 (1998).
[13] F. Muntean, M. S. Taylor, A. B. McCoy, and W. C. Lineberger, J. Chem. Phys. **121**, 5676 (2004).
[14] M. S. Taylor, Ph.D. thesis, University of Colorado, Boulder, 2004.
[15] G. J. Rathbone, T. Sanford, D. Andrews, and W. C. Lineberger, Chem. Phys. Lett. (in press).
[16] F. Misaizu, K. Tsukamoto, M. Sanekata, and K. Fuke, Surf. Rev. Lett. **3**, 405 (1996).
[17] F. Misaizu, K. Tsukamato, M. Sanekata, and K. Fuke, Laser Chem. **15**, 195 (1995).
[18] H. Hess, S. Kwiet, L. Socaciu, S. Wolf, T. Leisner, and L. Wöste, Appl. Phys. B: Lasers Opt. **71**, 337 (2000).
[19] T. Leisner, S. Vajda, S. Wolf, L. Wöste, and R. S. Berry, J. Chem. Phys. **111**, 1017 (1999).
[20] D. W. Boo, Y. Ozaki, L. H. Andersen, and W. C. Lineberger, J. Phys. Chem. A **101**, 6688 (1997).
[21] S. Wolf, G. Sommerer, S. Rutz, E. Schreiber, T. Leisner, L. Wöste, and R. S. Berry, Phys. Rev. Lett. **74**, 4177 (1995).
[22] H. Hess, K. R. Asmis, T. Leisner, and L. Wöste, Eur. Phys. J. D **16**, 145 (2001).
[23] M. S. Taylor, F. Muntean, W. C. Lineberger, and A. B. McCoy, J. Chem. Phys. **121**, 5688 (2004).
[24] M. Roeselová, U. Kaidor, and P. Jungwirth, J. Phys. Chem. A **104**, 6523 (2000).
[25] M. Roeselová, M. Mucha, B. Schmidt, and P. Jungwirth, J. Phys. Chem. A **106**, 12229 (2002).
[26] C.-G. Zhan and S. Iwata, Chem. Phys. Lett. **232**, 72 (1995).
[27] P. J. Campagnola, L. A. Posey, and M. A. Johnson, J. Chem. Phys. **95**, 7998 (1991).
[28] V. Vorsa, P. J. Campagnola, S. Nandi, M. Larsson, and W. C. Lineberger, J. Chem. Phys. **105**, 2298 (1996).
[29] W. C. Wiley and I. H. McLaren, J. Mass Spectrom. **32**, 4 (1997).
[30] M. J. Frisch, G. W. Trucks, H. B. Schlegel *et al.*, GAUSSIAN 98 (Gaussian, Inc., Pittsburgh, PA, 1998).
[31] M. J. Frisch, G. W. Trucks, H. B. Schlegel *et al.*, GAUSSIAN 03 (Gaussian, Inc., Pittsburgh, PA, 2003).
[32] X.-B. Wang, L.-S. Wang, R. Brown, P. Schwerdtfeger, D. Schröder, and H. Schwarz, J. Chem. Phys. **114**, 7388 (2001).
[33] M. Dolg, U. Wedig, H. Stoll, and H. Preuss, J. Chem. Phys. **86**, 866 (1987).
[34] R. A. Kendall, T. H. Dunning, Jr., and R. J. Harrison, J. Chem. Phys. **96**, 6796 (1992).
[35] T. H. Dunning, Jr., J. Chem. Phys. **90**, 1007 (1989).
[36] J. R. Reimers, R. O. Watts, and M. L. Klein, Chem. Phys. **64**, 95 (1982).
[37] L. A. Curtiss, D. J. Frurip, and M. Blander, J. Chem. Phys. **71**, 2703 (1979).
[38] In the $Cu(H_2O)$ study (Ref. 13), the Cu^+ and $Cu^+(H_2O)$ transients were fit to the following functions: $Cu^+(t)=I_1\{0.5+0.5\tanh[(t-t_0)/t_1]\}+I_2[1-\exp(-t/t_2)]+I_3[1-\exp(-t/t_3)]$ $Cu^+(H_2O)(t)=I_2\exp(-t/t_2)+I_3\exp(-t/t_3)$, where $I_1=0.35$, $I_2=0.5$, $I_3=0.15$, $t_0=0.4$ ps, $t_1=0.6$ ps, $t_2=8$ ps, and $t_3=100$ ps. In order to compare the Cu^+ and $Cu^+(H_2O)$ resulting from $Cu^-(H_2O)$ and $Cu^-(H_2O)_2$, the t_3 term is subtracted from the $Cu(H_2O)$ data and the resulting signals rescaled to match those from $Cu^-(H_2O)_2$.
[39] See EPAPS Document No. E-JCPSA6-122-003504 for (1) the geometrical parameters and (2) harmonic vibrational frequencies of the anion, neutral and cation $Cu(H_2O)_2$ stationary points. A direct link to this document may be found in the online article's HTML reference section. The document may also be reached via the EPAPS homepage (http://www.aip.org/pubservs/epaps.html) or from ftp.aip.org in the directory /epaps/. See the EPAPS homepage for more information.
[40] J. M. L. Martin and A. Sundermann, J. Chem. Phys. **114**, 3408 (2001).
[41] K. Pierloot, B. Dumez, P.-O. Widmark, and B. O. Roos, Theor. Chim. Acta **90**, 87 (1995).
[42] P. Ayotte, S. B. Nielsen, G. H. Weddle, M. A. Johnson, and S. S. Xantheas, J. Phys. Chem. A **103**, 10665 (1999).
[43] P. Ayotte, G. H. Weddle, J. Kim, and M. A. Johnson, Chem. Phys. **239**, 485 (1998).
[44] S. S. Xantheas and T. H. Dunning, Jr., Adv. Mol. Vib. Collision Dyn. **3**, 281 (1998).
[45] H. M. Lee and K. S. Kim, J. Chem. Phys. **114**, 4461 (2001).
[46] R. W. Gora, S. Roszak, and J. Leszczynski, Chem. Phys. Lett. **325**, 7 (2000).
[47] J. Kim, H. M. Lee, S. B. Suh, D. Majumdar, and K. S. Kim, J. Chem. Phys. **113**, 5259 (2000).
[48] M. Kowal, R. W. Gora, S. Roszak, and J. Leszczynski, J. Chem. Phys. **115**, 9260 (2001).
[49] S. Roszak, M. Kowal, R. W. Gora, and J. Leszczynski, J. Chem. Phys. **115**, 3469 (2001).
[50] H. E. Dorsett, R. O. Watts, and S. S. Xantheas, J. Phys. Chem. A **103**, 3351 (1999).
[51] S. S. Xantheas, J. Phys. Chem. **100**, 9703 (1996).
[52] The incremental H_2O dissociation energies from $Cu^-(H_2O)_n$ are derived

using the thermochemical cycle: $D_0[Cu^- - H_2O] = DE[Cu - H_2O] + VDE[Cu^-(H_2O)] - EA[Cu]$ $D_0[Cu^-(H_2O) - H_2O] = DE[Cu(H_2O) - H_2O] + VDE[Cu^-(H_2O)_2] - VDE[Cu^-(H_2O)]$, where EA[Cu] is the electron affinity of atomic copper; $VDE[Cu^-(H_2O)_n]$ is the measured vertical detachment energy of $Cu^-(H_2O)_n$; and $DE[Cu–H_2O]$ and $DE[Cu(H_2O)–H_2O]$ are the energies required to dissociate one H_2O molecule from neutral $Cu(H_2O)$ and $Cu(H_2O)_2$ starting from the corresponding anion equilibrium geometries. These energies are calculated to be $DE[Cu–H_2O] = 0.04$ eV and $DE[Cu(H_2O)–H_2O] = 0.13$ eV. This yields $D_0[Cu^- - H_2O] = 0.38 \pm 0.02$ eV and $D_0[Cu^-(H_2O)–H_2O] = 0.50 \pm 0.02$ eV.

[53] In the previous study of $Cu(H_2O)_1$ dynamics (Ref. 13), comparison of the simulated signals, derived from the quantum wavepacket calculations, with the experimental signals suggested a temperature range of 100–200 K for the precursor anions, and we extrapolate this temperature to the anions in the present study.

[54] L. A. Curtiss and E. Bierwagen, Chem. Phys. Lett. **176**, 417 (1991).

[55] N. F. Dalleska, K. Honma, L. S. Sunderlin, and P. B. Armentrout, J. Am. Chem. Soc. **116**, 3519 (1994).

[56] C. W. Bauschlicher, Jr., S. R. Langhoff, and H. Partridge, J. Chem. Phys. **94**, 2068 (1991).

[57] M. Rosi and C. W. Bauschlicher, Jr., J. Chem. Phys. **90**, 7264 (1989).

[58] M. Rosi and C. W. Bauschlicher, Jr., J. Chem. Phys. **92**, 1876 (1990).

[59] D. Feller, E. D. Glendening, and W. A. de Jong, J. Chem. Phys. **110**, 1475 (1999).

[60] A. M. El-Nahas, N. Tajima, and K. Hirao, J. Mol. Struct.: THEOCHEM **469**, 201 (1999).

[61] *Ab initio* calculations suggest that, as the second H_2O does not strongly interact with Cu, photons of similar energy will ionize both $Cu(H_2O)$ and $Cu(H_2O)_2$.

[62] W. H. Robertson, J. A. Kelley, and M. A. Johnson, Rev. Sci. Instrum. **71**, 4431 (2000).

[63] E. R. Barthel, I. B. Martini, and B. J. Schwartz, J. Phys. Chem. B **105**, 12230 (2001).

[64] I. B. Martini, E. R. Barthel, and B. J. Schwartz, J. Chem. Phys. **113**, 11245 (2000).

[65] E. R. Barthel, I. B. Martini, and B. J. Schwartz, J. Chem. Phys. **112**, 9433 (2000).

[66] J. A. Kloepfer, V. H. Vilchiz, V. A. Lenchenkov, and S. E. Bradforth, Chem. Phys. Lett. **298**, 120 (1998).

[67] J. A. Kloepfer, V. H. Vilchiz, V. A. Lenchenkov, A. C. Germaine, and S. E. Bradforth, J. Chem. Phys. **113**, 6288 (2000).

[68] V. H. Vilchiz, J. A. Kloepfer, A. C. Germaine, V. A. Lenchenkov, and S. E. Bradforth, J. Phys. Chem. A **105**, 1711 (2001).

[69] L. Lehr, M. T. Zanni, C. Frischkorn, R. Weinkauf, and D. M. Neumark, Science **284**, 635 (1999).

[70] D. Serxner, C. E. H. Dessent, and M. A. Johnson, J. Chem. Phys. **105**, 7231 (1996).

[71] C. E. H. Dessent, J. Kim, and M. A. Johnson, Acc. Chem. Res. **31**, 527 (1998).

[72] C. E. H. Dessent, M. A. Johnson, I. Becker, and O. Cheshnovsky, Electron Transfer-from Isolated Molecules to Biomolecules, Pt 1 **106**, 265 (1999).